Wavelet-Domain Color Image Enhancement Using Filtered Directional Bases and Frequency-Adaptive Shrinkage

Sangjin Kim, Wonseok Kang, Eunsung Lee, and Joonki Paik, *Member*, IEEE

Abstract — *This paper presents a novel wavelet-domain color image enhancement using filtered directional bases and frequency-adaptive shrinkage. Most traditional noise reduction methods tend to over-suppress high-frequency details. For overcoming this problem we first decompose the input image into flat and edge regions, and remove noise using the alpha map computed from wavelet transform coefficients of LH, HL, and HH bands. After removing noise in the flat region, we further remove noise in edge regions by adaptively shrinking wavelet coefficients based on the entropy. Moreover, we present a new directional transform using wavelet basis and Gaussian low pass filters. The wavelet coefficients of edge regions are inverse transformed by using the filtered wavelet bases. Experimental results show the proposed algorithm can reduce noise without losing sharp details and is suitable for commercial low-cost imaging systems, such as digital cameras, CCTV, and surveillance system[1].*

Index Terms — noise reduction, image denoising, wavelet transform, entropy analysis.

I. INTRODUCTION

In recent times, the single-sensor color imaging technology has become more popular in various applications, such as digital still cameras, camcorders, mobile phone cameras, and surveillance video cameras. Among various image processing techniques, noise reduction is the most important for enhancing color images. The sensor output carries both signal and noise components which make high-quality image acquisition difficult. Especially, color images acquired by a single-sensor camera are subject to various types of noise. For this reason it is of paramount importance to reduce noise without affecting sharp details of an image [1].

Because of the commonality of noise reduction methods in most image and video systems, there has been a large amount of research dedicated image denoising over the past several decades. Existing noise filtering methods include variable coefficient linear filters [2], [3], adaptive nonlinear filters [4], [5], iterative methods [6], [7], discrete cosine transform (DCT) based methods [8], and cluster filtering [9], to name a few.

These denoising algorithms, however, tend to attenuate original signal features. [5], [10], [11]. In order to overcome this problem, the discrete wavelet transform (DWT) has been used to suppress noise in digital images. Wavelet-based image denoising algorithms generally consist of three steps; i) wavelet transform of the input noisy image, ii) shrinking a selective part of wavelet coefficients, and iii) inverse wavelet transform of the modified coefficients. Based on this framework, there are two types of wavelet-based noise reduction methods; one is to seek appropriate wavelet basis for higher frequency resolution and the other is to select more appropriate wavelet coefficients to be shrunk [12].

For the first type, many directional wavelet transforms have been developed under the multi-scale analysis framework, including steerable wavelets, wedgelets, curvelets, contourlets, and directionalets [12]. While these methods can accurately represent pointwise singularities, they are weak in representing other discontinuities such as contours and edge in images [13].

For the second type, many wavelet shrinkage methods have been developed for denoising, such as SureShrink, BayesShrink, and VisuShrink. These methods have advantage of exploiting the dependency between coefficients. However, it tends to lose sharp details [12].

Based on the above observations, we propose a novel wavelet-based noise reduction algorithm which uses both enhanced directional wavelet bases and multivariate shrinkage method. More specifically, we present a new directional transform using combined wavelet functions and adaptive Gaussian low pass filter. And the proposed shrinkage method modifies the wavelet transform coefficients based on local variance in flat regions, while it employs entropy computation in high-frequency regions.

This paper is organized as follows. In section 2, we briefly describe theoretical background of wavelet-based noise reduction. The proposed wavelet-domain noise reduction algorithm is presented in section 3. In Section 4, we present experimental results, and section 5 concludes the paper.

Sangjin Kim is with the Department of Image Engineering, Chung-Ang University, Seoul, Korea. (e-mail: layered372@wm.cau.ac.kr).

Wonseok Kang is with the Department of Image Engineering, Chung-Ang University, Seoul, Korea. (e-mail: kandws12@wm.cau.ac.kr).

Eunsung Lee is with the Department of Image Engineering, Chung-Ang University, Seoul, Korea. (e-mail: lessel7@wm.cau.ac.kr).

Joonki Paik is with the Department of Image Engineering, Chung-Ang University, Seoul, Korea. (e-mail: paikj@cau.ac.kr).

II. THEORETICAL BACKGROUND

A. Noise Modeling

The dominant type of noise in digital images is usually modeled as the additive zero-mean white Gaussian noise (AWGN) process. The probability density function (PDF) of a Gaussian random variable, x, is given as

$$G(x) = \frac{1}{\sqrt{2\pi}\sigma} e^{-\frac{(x-\bar{x})^2}{2\sigma^2}}, \tag{1}$$

where x represents the intensity value, $\bar{x}$ is the mean value of x, and σ is the standard deviation.

The noisy image model is expressed as

$$g(i,j) = f(i,j) + N(i,j), \tag{2}$$

where g and f respectively represent noisy and noise-free images, and $N(i,j)$ is the AWGN noise.

B. Multi-resolution analysis using the discrete wavelet transform

The discrete wavelet transform (DWT) passes the input signal through a series of filters. A signal can be decomposed into a set of band-limited components, called sub-bands, which can be reassembled to completely reconstruct the original image. Let $h_0(n)$ and $h_1(n)$ be analysis filters, and $g_0(n)$ and $g_1(n)$ be synthesis filters. As shown in Fig. 1, the output of the low-pass filter $h_0(n)$ represents an approximation of $x(n)$, and the output of the high-pass filter $h_1(n)$ represents a detail part of $x(n)$. Both outputs can be down-sampled without loss of information because the bandwidth is reduced by low-pass and high-pass filterings.

The reconstructed signal $\hat{x}(n)$ is obtained by adding the up-sampled and filtered version of $y_0(n)$ and $y_1(n)$. For error-free construction, in other words $\hat{x}(n) = x(n)$, the following conditions must be satisfied.

$$H_0(-z)G_0(z) + H_1(-z)G_1(z) = 0,$$
$$H_0(z)G_0(z) + H_1(z)G_1(z) = 2, \tag{3}$$

where $H_i(z)$ and $G_i(z)$ respectively represents z-transforms of $h_i(n)$ and $g_i(n)$, $i \in \{0,1\}$. We call (3) the conditions for perfect reconstruction, whose detailed derivation can be found in [1].
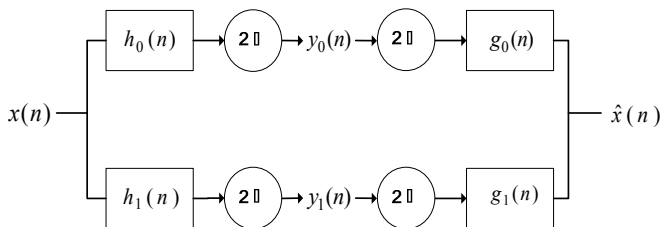

Fig. 1. A two-band filter bank.

After several algebraic steps, the perfect reconstruction condition is expressed as the following biorthogonality constraint

$$\langle h_i(2n-k), g_j(k) \rangle = \delta(i-j)\delta(n), \quad i,j \in \{0,1\}, \tag{4}$$

which is imposed to analysis and synthesis filters of all two-band, real-coefficient, perfect reconstruction filter banks.

If the filters are further constrained to be orthonomal, such as

$$\langle g_i(n), g_j(n+2m) \rangle = \delta(i-j)\delta(m), \quad i,j \in \{0,1\}, \tag{5}$$

given a synthesis low-pass filter g_0, impulse responses h_0, h_1 and g_1 are determined as

$$g_1(n) = (-1)^n g_0(2K-1-n),$$
$$h_i(n) = g_i(2K-1-n), \quad i \in \{0,1\}, \tag{6}$$

where $2K$ represents the length of each filter.

Given one-dimensional (1D) scaling and wavelet functions, such as $\varphi(x)$ and $\psi(x)$, which satisfy the following as [3]

$$\varphi(x) = \sum_n h_\varphi(n)\sqrt{2}\varphi(2x-n),$$
$$\psi(x) = \sum_n h_\psi(n)\sqrt{2}\varphi(2x-n), \tag{7}$$

where $h_\varphi(n)$ and $h_\psi(n)$ respectively represent scaling and wavelet function coefficients.

The corresponding two-dimensional (2D) scaling and three wavelets are formulated by separable combinations of 1D scale and wavelet functions. Based on the complexity of hardware, there are three different modes for processing the digital camera image, such as:

$$\phi(x,y) = \phi(x)\phi(y),$$
$$\psi^H(x,y) = \psi(x)\phi(y),$$
$$\psi^V(x,y) = \phi(x)\psi(y),$$
$$\psi^D(x,y) = \psi(x)\psi(y). \tag{8}$$

The 2D DWT is given as

$$W_\phi(j_0,m,n) = \frac{1}{\sqrt{MN}} \sum_{x=0}^{M-1}\sum_{y=0}^{N-1} f(x,y)\phi_{j_0,m,n}(x,y),$$
$$W_\psi^i(j,m,n) = \frac{1}{\sqrt{MN}} \sum_{x=0}^{M-1}\sum_{y=0}^{N-1} f(x,y)\psi^i_{j,m,n}(x,y), \tag{9}$$
$$i \in \{H,V,D\},$$

where j_0 represents an arbitrary starting scale, $W_\varphi(j_0,m,n)$ is coefficients of the approximation of $f(x,y)$ at scale j_0, and $W_\psi^i(j,m,n)$ is coefficients of three directional (horizontal, vertical, and diagonal) details for scales $j \geq j_0$. Fig. 2 shows the wavelet transform [1].
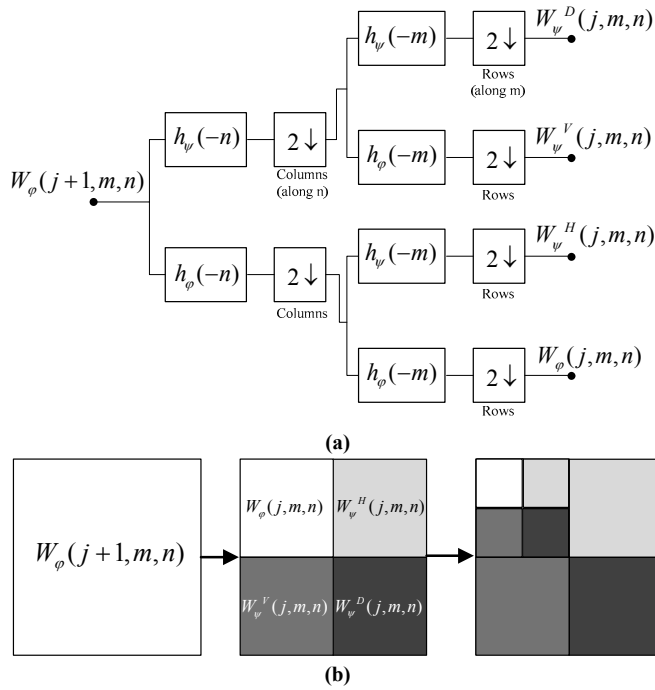
(a)

(b)

Fig. 2. The 2D DWT: (a) the analysis filter bank and (b) the resulting decomposition of the input image.

C. Entropy Analysis

In order to determine the amount of noise, we analyze the entropy of wavelet coefficients in the following manner

$$E_{W_\psi^i} = \sum_{k \in B} p_k \ln p_k, \ for \ i = \{H, V, D\}, k = 1, \cdots, MN \quad (10)$$

where B represent an $M \times N$ local block in the wavelet sub-band, $E_{W_\psi^i}$ represent the entropy of the local block, k is a number of wavelet coefficients in the corresponding block, and p_k is a probability of wavelet coefficients. After filtering noise in flat regions, we need to remove noise in the neighborhood of edges. To this end we compute entropy as a measure of both complexity and energy of an image.

III. PROPOSED WAVELET-DOMAIN NOISE REDUCTION ALGORITHM

A typical image formation system of a digital camera consists of; (i) a set of optical lenses, (ii) the analog front end (AFE) module including a color filter array (CFA), an image
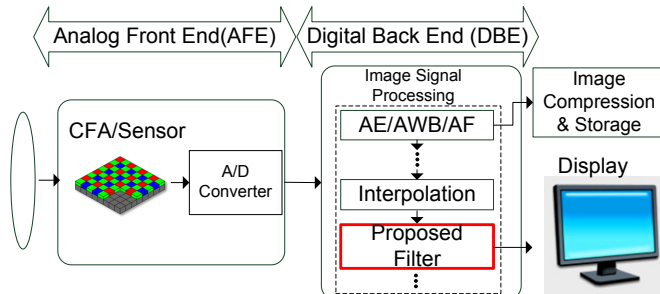
sensor, an analog-to-digital converter (ADC), and additional analog circuitry, (iii) the digital back end (DBE) module including various digital signal processing blocks, and (iv) the storage and display devices, as shown in Fig. 3. The proposed noise removing filter belongs to the DBE module in the image formation system.

The proposed noise removing algorithm is shown in Fig. 4, where wavelet transform coefficients are used to compute the alpha map. We then decompose the flat and the edge regions for adaptive noise filtering. Finally, we compose a new directional transform using combined wavelet functions and adaptive Gaussian low pass filter.

A. Adaptive Image Classification

In order to classify the strong edge and pure noise regions, we compute the alpha-map using local variance in the low-pass sub-band wavelet coefficients. We compute local variance at each pixel (x, y) as

$$v(x, y) = \frac{1}{PQ} \sum_{(x,y) \in S} \left(f(x, y) - m_{xy} \right)^2, \quad (11)$$

where S represents a rectangular region encompassing (x, y), $f(x, y)$ is the pixel value at (x, y), P and Q are respectively vertical and horizontal sizes of the region, and m_{xy} is the local mean of the region as

$$m_{xy} = \frac{1}{PQ} \sum_{(x,y) \in S} f(x, y). \quad (12)$$

We compute the weighting factor α in the following manner as

$$\alpha(x, y) = \frac{1}{1 + \sigma v(x, y)}, \quad (13)$$

where the tuning parameter σ is chosen so that α distributes as uniformly as possible in [0,1]. For the best normalized α, a typical value of σ is experimentally equal to 200. Depending on the amount of noise, σ is adjustable. For classification of flat(pure noise) and edge regions, α-map is used as

$$r_{flat}(m, n) = \alpha W_\psi^i(m, n)$$
$$r_{edge}(m, n) = (1 - \alpha) W_\psi^i(m, n), \ for \ 0 < \alpha < 1, i = \{H, V, D\} \quad (14)$$

Fig. 3. The image signal processing chain of a digital camera with the proposed noise removing filter.
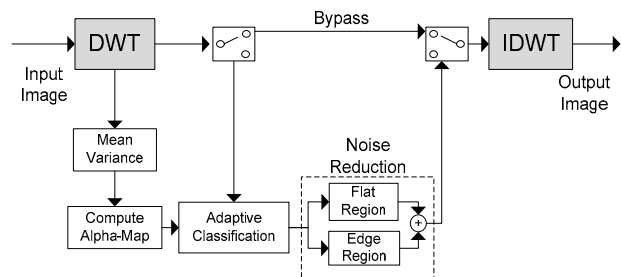

Fig. 4. The proposed noise reduction framework.

where $W_\psi{}^i$ represents three direction sub-bands, $i \in \{H, V, D\}$, m and n vertical and horizontal sizes of the sub-band. As indicated by (14), wavelet coefficients are shared the flat regions r_{flat} with the edge region r_{edge}. We shrink wavelet coefficients using each other method.

B. Noise Reduction in the Flat Region by Wavelet Shrinkage

Thresholding transform coefficients are widely used for signal denoising. The thresholding method removes additive noise by eliminating or reducing transform coefficients corresponding to the basis function belonging to noise. This primary advantage of this method is simplicity and economical implementation. However, it cannot fully utilize the frequency localization property of wavelet bases. So, we propose adaptive wavelet shrinkage method by using spatial information.

It is well known that the human visual system is sensitive to additive noise in the edge region more than the flat region. So, we need to shrink wavelet coefficients in the flat region as much as possible. More specifically, wavelet coefficients in the flat region are inner-producted by the α-map in the detail sub-band. As a result, noise can be reduced in flat regions. In red channel, the result of proposed wavelet shrinkage in flat the region is shown in Fig. 5.

C. Entropy-Adaptive Noise Reduction in the Edge Region

After filtering noise in the flat region, we need to remove noise in the neighborhood of edge. To this end we compute entropy as a measure of both complexity and energy of an image. Combination of the entropy and wavelet's directional frequency property can completely localize features in the spatial-frequency domain [20]. More specifically, local entropy of each wavelet coefficients in r_{edge} contains information of local complexity in the high-frequency region.

Because a noisy edge region has higher complexity than purely noisy region, a sub-band with higher entropy can be
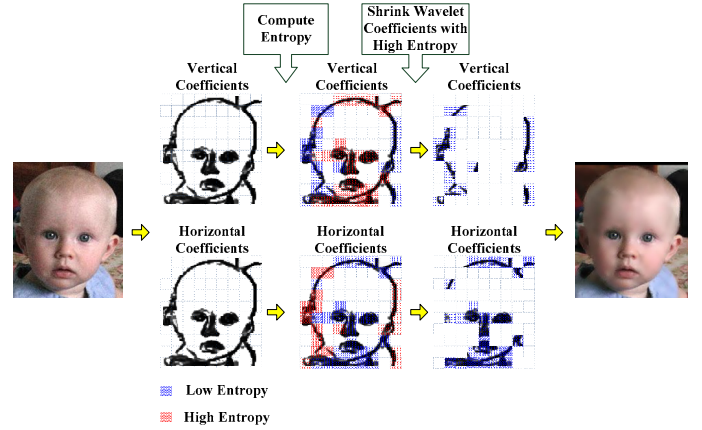

Fig. 6. The proposed entropy-adaptive noise reduction algorithm in the edge region.

considered to contain more noise than other sub-bands. Based on this analysis we can reduce noise by shrinking wavelet coefficients with high entropy. The proposed noise reduction algorithm is depicted in Fig. 6.

D. Filtering of Wavelets

After selecting 1D scaling $\phi(x)$ and wavelet functions $\psi(x)$, we can generate a 2D scaling function and three 2D directional wavelet functions using (8). Fig. 7 shows a set of 1D, 8-tab symlet filters that satisfy the condition of 1D scaling and wavelet functions given in (7). The resulting four 2D wavelets using the 1D symlet filters are shown in Fig. 8.

The filtered version of four 2D wavelets is given by convolving with the Gaussian low pass filter, as

$$
\begin{aligned}
\phi_V(x,y) &= \phi(x)\phi(y), \\
\psi^H{}_V(x,y) &= \psi(x)\{h_G(y)*\varphi(y)\}, \\
\psi^V{}_V(x,y) &= \{h_G(x)*\phi(x)\}\psi(y), \\
\psi^D{}_V(x,y) &= \{h_G(x)*\psi(x)\}\{h_G(y)*\psi(y)\},
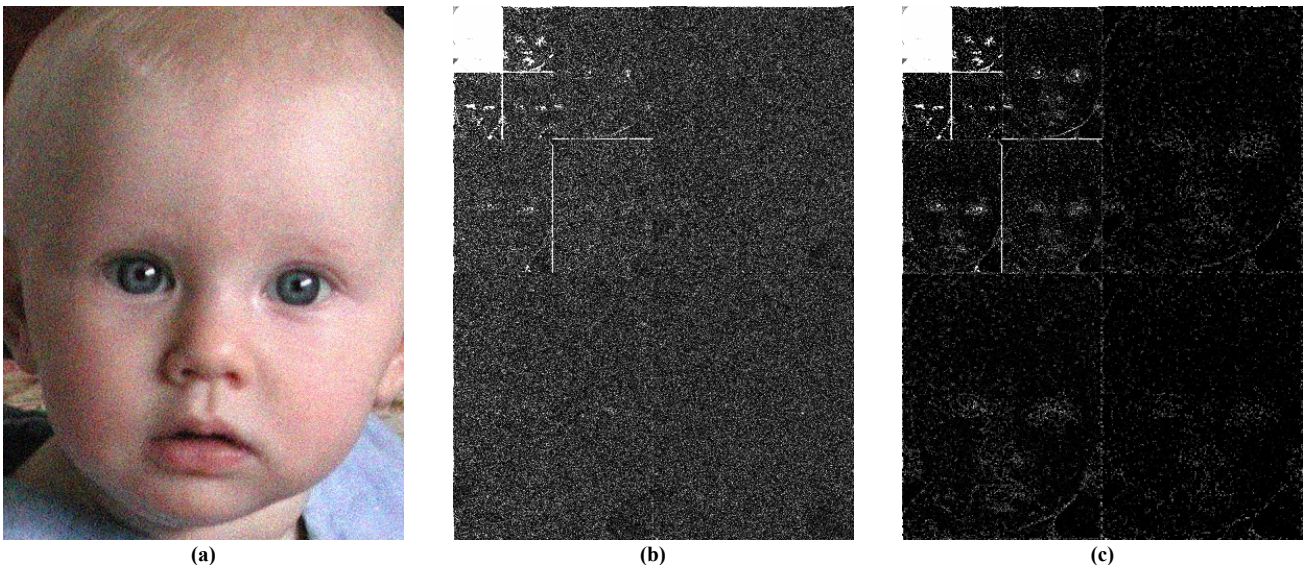\end{aligned}
\tag{15}
$$

Fig. 5. Results of noise reduction by shrinking wavelet coefficients: (a) the input noisy image, (b) wavelet transform of (a) (red-channel), and (c) shrinked wavelet coefficients using proposed method.
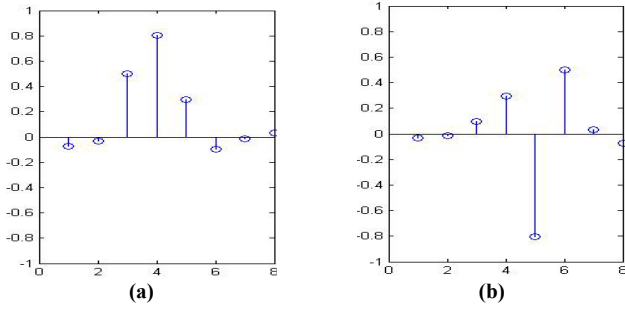
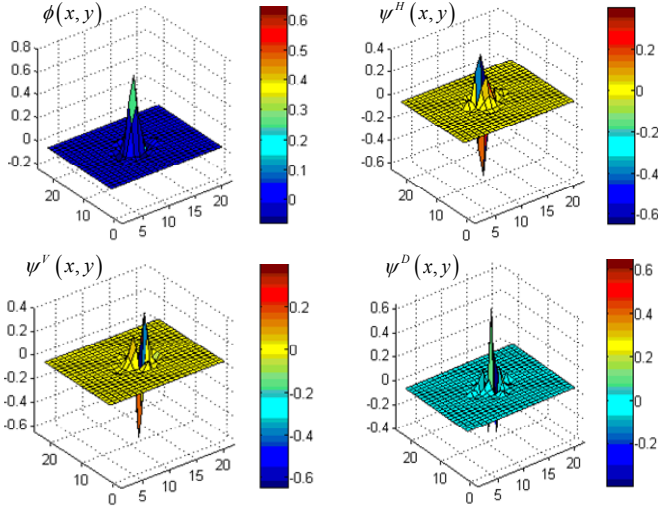Fig. 7. 1D, 8-tab symlet filters: (a) scaling and (b) wavelet functions.

Fig. 8. 2D wavelet functions generated by the relationships in (8) using 1D symlet functions given in Fig. 7.
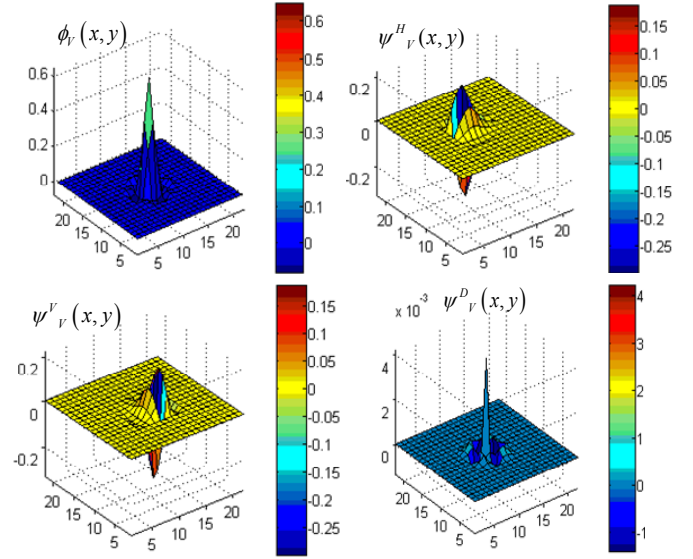

Fig. 9. The filtered version of 2D symlet wavelets.

proposed algorithm is better in both suppressing noise and preserving sharp details. Performance comparison using the PSNR values and the CPU computation time in seconds obtained by several existing denoising algorithms [16], [21], [22], is given in Tables I and II, respectively.

V. CONCLUSION

In this paper, we proposed novel wavelet-domain color image enhancement using filtered directional bases and

where h_G represents the Gaussian low-pass filter whose bandwidth is smaller than that of wavelet basis, and * indicates convolution. The resulting filtered wavelets using (15) are shown in Fig. 9.

Depending on the amount of noise in each block, an appropriate portion of filtered bases is applied. By inverse transforming wavelet coefficients using the filtered wavelets the remaining noise can further be reduced.

IV. EXPERIMENTAL RESULTS

For evaluating the performance of the proposed algorithm, we used a set of standard images of size 768x512, and outdoor test images of size 1504x1000 acquired by using a digital single lens reflected (DSLR) camera. The performance of the proposed noise reduction framework is evaluated with peak-to-peak signal-to-noise ratio (PSNR) and the CPU computation time in seconds on a PC equipped with 2.66 GHz CPU, and 8GB RAM memory.

Experimental results of the proposed method for natural noisy images are shown in Fig. 10. For the natural images shown in Fig. 10, the proposed method efficiently removes noise and at the same time preserves the edge details. In order to measure the objective performance, we add synthetic noise (standard deviation $\sigma = 20$) to original test images. The results of proposed method and NAST filter [16] are shown in Fig. 11. Based in the comparison with NAST filter, the
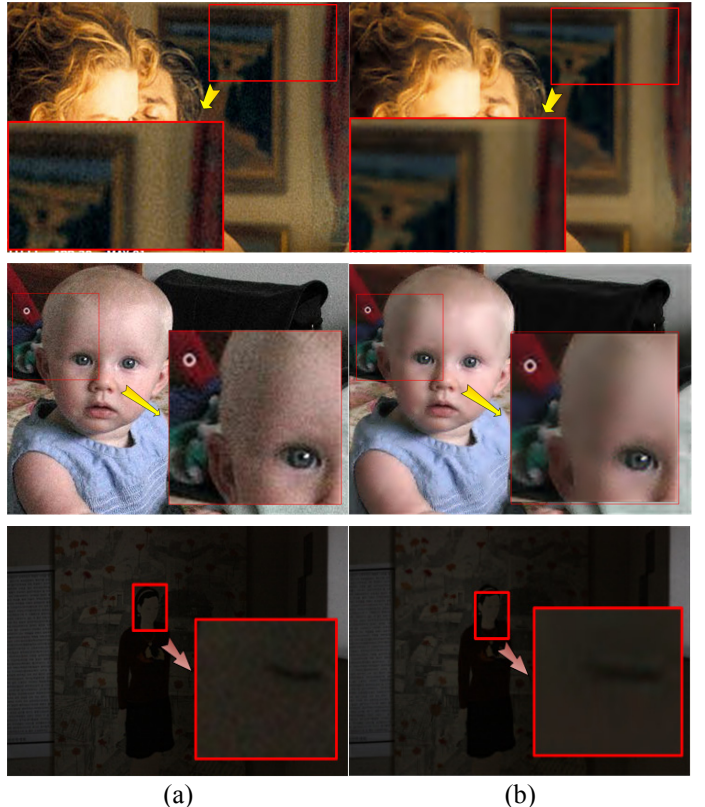

Fig. 10. Experimental results using the proposed method: (a) Natural images and (b) Enhanced images using the proposed method.

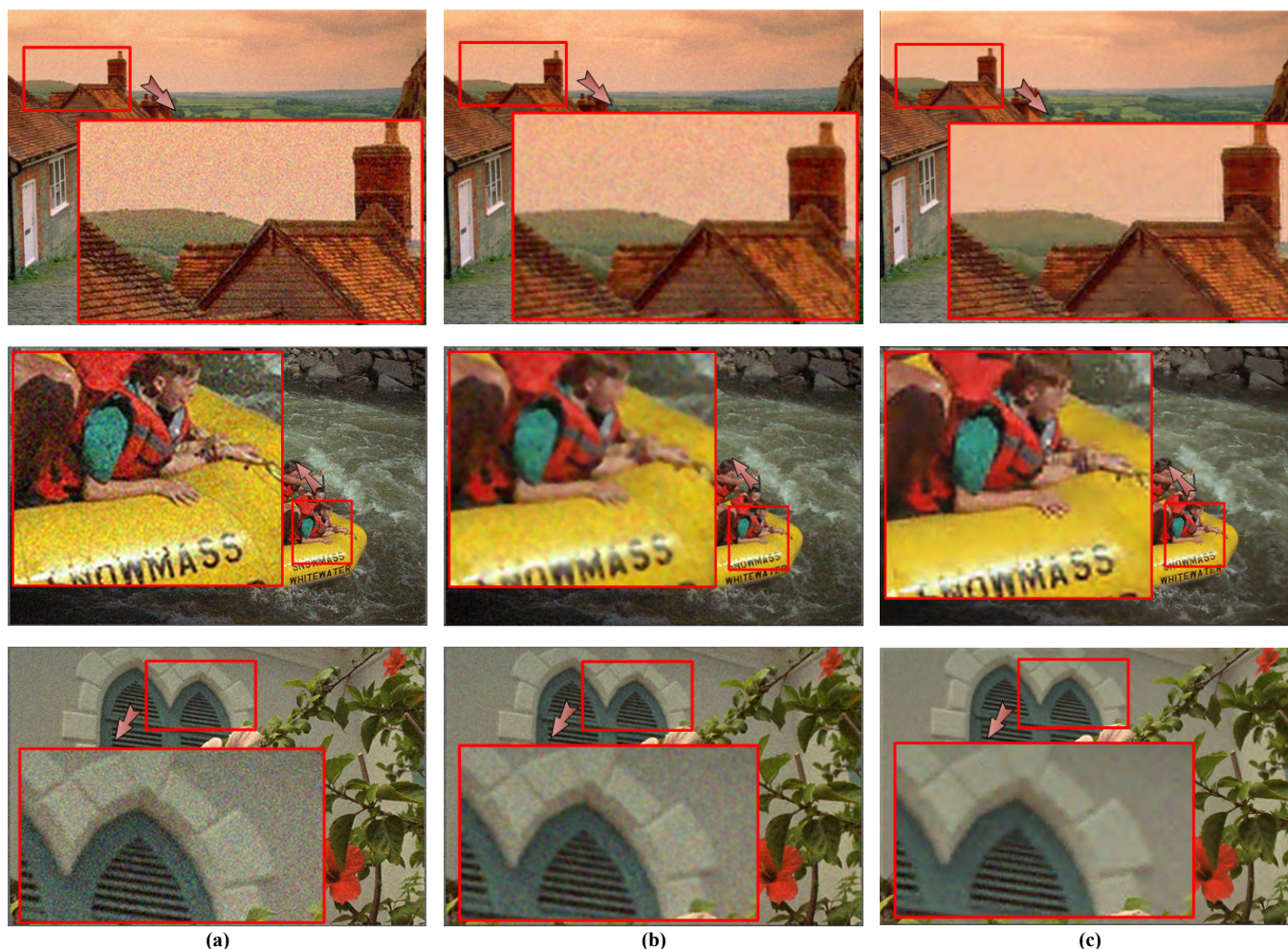**Fig. 11. Simulation results using standard images using NAST filter [17] and the proposed method for noise with (σ =20): (a) noisy images, (b) results of NAST filter, and (c) results of the proposed algorithm.**

TABLE I
PERFORMANCE COMPARISON OF THE PROPOSED AND EXISTING ALGORITHMS

Input Image (768x512)	Denoising Type	Noise Value(σ)				
		5	10	15	20	25
	NAST [16]	27.8323	27.3555	26.8109	26.1125	25.8976
	DFB-GSM [21]	28.5656	28.2200	27.3500	26.5400	26.3500
	CWM [22]	27.5422	27.0722	26.1100	26.6000	25.6500
	Proposed Algorithm	28.9282	28.0934	27.9679	27.0393	26.5434
	NAST [16]	27.4012	26.9699	26.3920	25.7119	25.0150
	DFB-GSM [21]	32.2124	31.1800	30.2100	28.9000	28.6000
	CWM [22]	26.6785	25. 3054	25.1600	25.0200	24.1380
	Proposed Algorithm	31.3129	31.1872	31.0928	30.6594	29.0124
	NAST [16]	31.5422	30.5097	29.2734	28.0460	26.9873
	DFB-GSM [21]	32.2124	31.1800	30.2100	28.9000	28.6000
	CWM [22]	26.6785	25. 3054	25.1600	25.0200	24.1383
	Proposed Algorithm	32.0753	31.6743	30.7567	29.3680	28.9933
	NAST [16]	28.1202	31.2181	29.2734	28.0460	26.9873
	DFB-GSM [21]	33.5124	32.7218	30.9988	29.2892	29.1209
	CWM [22]	28.3123	29. 2913	29.1299	29.0002	27.9558
	Proposed Algorithm	30.0021	32.3021	32.0022	33.6324	29.9421
	NAST [16]	30.9212	30.0028	28.9952	27.9213	26.2821
	DFB-GSM [21]	31.4209	32.1174	30.2973	29.8623	28.4876
	CWM [22]	26.1298	25. 1148	24.7821	23.1932	22.6821

TABLE II
PERFORMANCE CPU COMPUTATION TIME IN SECONDS FOR THE PROPOSED AND EXISTING ALGORITHMS

| Input Image (1504x1000)	Denoising Type	Noise Value(σ)				Average
		20	30	40	50	
	NAST [16]	15.402	15.132	15.326	15.326	15.297
	DFB-GSM [21]	480.123	478.180	482.921	485.230	481.614
	CWM [22]	14.123	14.538	14.231	14.522	14.354
	Proposed Algorithm	10.222	11.142	10.921	10.823	10.777
	NAST [16]	14.911	14.923	14.824	14.997	14.9138
	DFB-GSM [21]	450.389	452.133	465.421	468.159	459.026
	CWM [22]	13.982	13.999	13.993	13.002	13.744
	Proposed Algorithm	10.913	10.124	10.524	10.776	10.584
	NAST [16]	15.482	15.990	15.332	15.132	15.484
	DFB-GSM [21]	460.132	459.782	461.123	462.124	460.790
	CWM [22]	14.009	13.782	13.791	13.832	13.854
	Proposed Algorithm	10.813	10.992	11.119	11.182	11.027
	NAST [16]	14.912	15.182	15.329	15.882	15.326
	DFB-GSM [21]	440.224	441.898	446.432	450.991	444.886
	CWM [22]	13.329	13.124	13.921	13.979	13.588
	Proposed Algorithm	10.992	10.998	11.145	11.331	11.117

frequency-adaptive shrinkage. More specifically, we present a new directional transform using combined wavelet functions and adaptive Gaussian low-pass filters. We also proposed the wavelet shrinkage method that modifies wavelet transform coefficients based on local variance in the flat regions and on entropy in high-frequency regions. The proposed method can efficiently reduce additive Gaussian noise which can be considered as the most popular type of noise in digital images. The proposed framework reduces noise without losing sharp details.

The proposed noise reduction algorithm overcomes limitations in traditional wavelet-based algorithms problem, and is suitable for real-time applications such as low cost camcorders, digital cameras, mobile phone camera, and surveillance video systems.

REFERENCES

[1] R. Gonzalez and R. Woods, *Digital image processing*, 2nd ed., PrenticeHall, 2001.

[2] R. Dugad and N. Ahuja, "Video denoising by combining Kalman and Wiener estimates," *IEEE Int. Conf. Image Processing*, vol. 4, pp. 152–156, October 1999.

[3] O. Ojo and T. Kwaaitaal "An algorithm for integrated noise reduction and sharpness enhancement," *IEEE Trans. Consumer Electronics*, vol. 46, no. 3, pp. 474-480, August 2000.

[4] G. Plonka and M. Jianwei, "Nonlinear regularized reaction-diffusion filters for denoisiong of image with textures," *IEEE Trans. Image Processing*, vol. 17, no. 8, pp. 1283 - 1294, August 2008.

[5] M. Zhang and B. Gunturk, "Multi-resolution bilateral filtering for image denoising," *IEEE Trans. Image Processing*, vol.17, no. 12, pp. 2324 – 2333, December 2008.

[6] C. Deledalle, L. Denis, and F. Tupin, "Iterative weighted maximum likelihood denoising with probabilistic patch-based weights," *IEEE Trans. Image Processing,* vol. 18, no. 12, pp. 2661-2672, December 2009.

[7] X. Jinjun and S. Osher, "Iterative regularization and nonlinear inverse scale space applied to wavelet-based denoising," *IEEE Trans. Image Processing,* vol. 16, no. 2, pp. 534 - 544, February 2007.

[8] S. Kim, S. Jang, M. Kim, and J. Ra, "Efficient block-based coding of noise images by combining pre-filtering and DCT," *IEEE Int. Symp. Circuits System*, vol. 4, pp. 37–40, June 1999.

[9] Y. Wong, E. Viscito, and E. Linzer, "Preprocessing of video signals for MPEG coding by clustering filter," *IEEE Int. Conf. Image Processing*, vol. 2, pp. 2129–2133, October 1995.

[10] J. Bai and X. Feng, "Fractional-order anisotropic diffusion for image denoising," *IEEE Trans. Image Processing*, vol. 16, no. 10, pp. 2492 – 2502, October 2007.

[11] J. Wang, Y. Guo, Y. Ying, Y. Liu, and Q. Peng, "Fast non-local algorithm for image denoising," *IEEE Int. Conf. Image Processing*, pp. 1429 – 1432, October 2006.

[12] Y. Jingyu, W. Yao, X. Wenli, and D. Qionghai, "Image and video denoising using adaptive dual-tree discrete wavelet packets," *IEEE Trans. Circuits and Systems for Video Technology*, vol. 19, no. 5, pp. 642 - 655, May 2009.

[13] M. Vetterli, "Wavelet, approximation, and compression," *IEEE Signal Processing Magazine*, vol. 18, no. 5, pp. 59–73, Sep. 2001.

[14] P. Shui, Z. Zhou, and J. Li, "Image denoising algorithm via best wavelet packet base using Wiener cost function," *IET Image Processing*, vol. 1, no. 3, pp. 311-318, September 2007.

[15] M. Mignotte, "Image denosing by averaging of piecewise constant simulations of image partitions," *IEEE Trans. Image Processing*, vol. 16, no. 2, pp. 523-533, February 2007.

[16] S. Lee, V. Maik, J. Jang, J. Shin, and J. Paik, "Noise-adaptive spatio-temporal filter for real-time noise removal in low light level images," *IEEE Trans. Consumer Electronics*, vol. 51, no. 2, pp. 648-653, May 2005.

[17] K. Hirakawa, M. Xiao, and P. Wolfe, "A framework for wavelet-based analysis and processing of color filter array images with applications to denoising and demosaicing," *IEEE ICASSP 2007*, vol. 1, pp. 597 – 600, April 2007.

[18] S. Rahman, M. Ahmad, and M. Swarmy, "Bayesian wavelet-based image denoising using the gauss–hermite expansion," *IEEE Trans. Image Processing*, vol. 17, no. 10, pp. 1755 – 1771, October 2008.

[19] Z. Lei, W. Xiaolin, and Z. David, "Color reproduction from noisy CFA data of single sensor digital cameras," *IEEE Trans. Image Processing*, vol. 16, no. 9, pp. 2184 – 2197, September 2007.

[20] H. Zheng, C. Xiaoqing, and L. Guoming, "Wavelet entropy measure definition and its application for transmission line fault detection and identification," *International Conference on Power System Technology 2006*, pp. 1 – 6, October 2006.

[21] J. Portilla, V. Strela, M. Wainwright, and E. Simoncelli, "Image denoising using scale mixtures of Gaussians in the wavelet domain," *IEEE Trans. Image Processing*, vol. 12, no. 11, pp. 1338–1351, December 2003.

[22] B. Song, and K. Chun, "Motion compensated noise estimation for efficient pre-filtering in a video encoder," *IEEE Int. Conf. Image Processing*, vol. 2, pp. 211-214, August, 2003.

BIOGRAPHIES
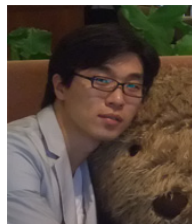
Sangjin Kim was born in Seoul, Korea in 1978. He received the B.S. degree in electronic engineering from Kangnam University, Korea, in 2003 and M.S degree in image processing from Chung-Ang University, Korea, in 2005.

Currently, he is pursuing Ph.D. degree in image processing at Chung-Ang University. His research interests include image restoration, computational camera, image and video processing, and real-time object tracking.

Wonseok Kang was born in Jeju, Korea in 1983. He received the B.S. degree in electronic engineering from Korea Aerospace University, Korea, in 2010.

Currently, he is pursuing M.S. degree in image processing at Chung-Ang University. His research interests include image restoration, computational camera and data fusion.

Eunsung Lee was born in Seoul, Korea in 1982. He received the B.S. degree in electronic engineering from Chung-Ang University, Korea, in 2009.

Currently, he is pursuing M.S. degree in image processing at Chung-Ang University. His research interests include image restoration, computational camera, and image enhancement.

Joonki Paik was born in Seoul, Korea in 1960. He received the B.S. degree in control and instrumentation engineering from Seoul National University in 1984. He received the M.S. and the Ph.D. degrees in electrical engineering and computer science from Northwestern University in 1987 and 1990, respectively.

After getting the Ph.D. degree, he joined Samsung Electronics, where he designed the image stabilization chip sets for consumer's camcorders. Since 1993, he has worked for Chung-Ang University, Seoul, Korea, where he is currently a Professor in the Graduate school of Advanced Imaging Science, Multimedia and Film. From 1999 to 2002, he was a visiting Professor at the Department of Electrical and Computer Engineering at the University of Tennessee, Knoxville. From 2005 to 2007 he served as Dean of the Graduate School of Advanced Imaging Science, Multimedia, and Film.

Dr. Paik is currently the head of the Image Processing and Intelligent Systems Laboratory, which is supported by the Brain Korea 21 Project, by the Korean Ministry of Information and Communication under ITRC-HNRC, and by Seoul Future Contents Convergence Cluster established by Seoul Research and Business Development (R&BD) Program.